arXiv:0910.3013v1 [hep-ex] 16 Oct 2009

Measurement of B_c^+ properties at CDF

T.S. Nigmanov[a]*, K.R. Gibson[b], M.P. Hartz[c], P.F. Shepard[b]
[a] *University of Michigan, Ann Arbor, MI 48109, USA*
[b] *University of Pittsburgh, Pittsburgh, PA 15260, USA and*
[c] *University of Toronto, Toronto M5S, Canada*

The B_c^+ meson is composed of two heavy quarks of distinct flavor. Measurements of its lifetime and production properties have been made based on semileptonic $B_c^+ \to J/\psi + l^+ + X$ decays using data collected with the CDF II detector corresponding to an integrated luminosity of 1 fb^{-1}. The B_c^+ average lifetime $c\tau$ is measured to be $142.5^{+15.8}_{-14.8}$(stat)$\pm 5.5(syst)$ μm. The measurements of the ratio of the production cross section times branching ratio of $B_c^+ \to J/\psi\mu^+\nu$ relative to $B^+ \to J/\psi K^+$ were done for two $p_T(B)$ thresholds: for $p_T(B) > 4$ GeV/c as 0.295 ± 0.040 (stat.)$^{+0.033}_{-0.026}$ (syst.) ± 0.036 (p_T spectrum) and for $p_T(B) > 6$ GeV/c as 0.227 ± 0.033 (stat.)$^{+0.024}_{-0.017}$ (syst.) ± 0.014 (p_T spectrum).

1. Introduction

The B_c^+ meson [1] is composed of an anti-bottom quark $\bar{b}$ and a charm quark c. The presence of two relatively heavy quarks with different flavors is unique to the B_c^+ system and affects the decay and production properties. The theoretically predicted lifetime [2] is about a factor of three times smaller than that of other B mesons. The expected B_c^+ production cross section [3] is about 3 orders of magnitude lower than the production cross section of the B^+ [4]. The first observation of the B_c^+ was made using data taken with the CDF detector at the Fermilab Tevatron during run I [5]. Precise mass measurements have been made by the CDF Collaboration using fully reconstructed $B_c^+ \to J/\psi\pi^+$ decays, where J/ψ decays through $J/\psi \to \mu^+\mu^-$ [6].

In this work we report preliminary measurements of the B_c^+ lifetime in the semileptonic decay modes $J/\psi\mu^+X$ and $J/\psi eX$, and the production cross section times branching ratio of the decay mode $B_c^+ \to J/\psi\mu^+\nu$ relative to the $B^+ \to J/\psi K^+$ decay. The results presented here are based on a data sample with an integrated luminosity of 1 fb^{-1} at $\sqrt{s}$=1.96 TeV collected by the CDF II detector.

2. The B_c^+ lifetime measurement concept

To measure the lifetime of the B_c^+, we construct a per event lifetime that is defined using variables measured in the transverse plane. If all of the decay products of the B_c^+ decay are identified, the lifetime ct is the lifetime of the B_c^+ meson in its rest frame measured in units of microns of light travel time. It is expressed as

$$ct = \frac{mL_{xy}}{p_T} \tag{1}$$

where m is the mass of the B_c^+, p_T is the momentum of the B_c^+ in the plane transverse to the direction of the proton beam, and L_{xy} is the decay length of the B_c^+ projected along the transverse momentum. The mass of the B_c^+ used in this measurement is $m = 6.286$ GeV/c^2 [6]. However, we do not measure all of the particles in the semileptonic B_c^+ final state. Instead we must define a pseudo lifetime

$$ct^* = \frac{mL_{xy}(J/\psi l^+)}{p_T(J/\psi l^+)} \tag{2}$$

where L_{xy} and p_T are evaluated using the $J/\psi + l^+$ system. We can obtain the true B_c^+ lifetime by defining a factor K, where $ct = Kct^*$. We evaluate the K factor distribution, $H(K)$, for B_c^+ events using Monte Carlo simulation. We are then able to express the distribution of ct^* for $B_c^+ \to J/\psi l^+X$ as

$$F_{B_c}(ct^*, \sigma) = \int dKH(K)\frac{K}{c\tau}\theta(ct^*)exp(-\frac{Kct^*}{c\tau}) \otimes G(\sigma) \tag{3}$$

where $c\tau$ is the average B_c^+ lifetime, σ represents the estimated error on the measurement of ct^* for each event, and $G(\sigma)$ is defined as

$$G(\sigma) = \frac{1}{\sqrt{2\pi}s\sigma}e^{-\frac{1}{2}(\frac{ct^*}{s\sigma})^2} \tag{4}$$

The measurement of the B_c^+ average lifetime is be carried out by minimizing $-2Log(L)$, which is evaluated for the candidate $J/\psi + l$ events. L is the likelihood function for the ct^* and σ measured in candidate events and includes $c\tau$ as a free parameter.

---

*Speaker, on behalf of the CDF Collaboration

3. The B_c^+ cross section measurement concept

We measure

$$\frac{\sigma(B_c^+)BF(B_c^+ \to J/\psi\mu^+\nu)}{\sigma(B^+)BF(B^+ \to J/\psi K^+)} = \frac{N(B_c^+)}{N(B^+)} \times \epsilon_{rel} \quad (5)$$

The basic strategy of the B_c^+ cross section measurement is to reconstruct the number of $B_c^+ \to J/\psi\mu^+\nu$ relative to the number of $B^+ \to J/\psi K^+$ candidates, $N(B_c^+)/N(B^+)$, determine the relative detector and reconstruction efficiency, $\epsilon_{rel} = \epsilon(B^+)/\epsilon(B_c^+)$, and use these to determine the ratio of the final production cross section times branching ratio.

4. The event selection

The analysis presented here is based on the events recorded with a di-muon trigger that is dedicated to $J/\psi \to \mu^+\mu^-$ decays. Both analysis use the same $J/\psi \to \mu^+\mu^-$ sample. The muon pair is reconstructed within a pseudo-rapidity range $|\eta| < 1.0$. We select about $6.9{\times}10^6$ J/ψ candidates, measured with a mass resolution of approximately 12 MeV/c^2. The di-muon invariant mass distribution is shown in Fig. 1.

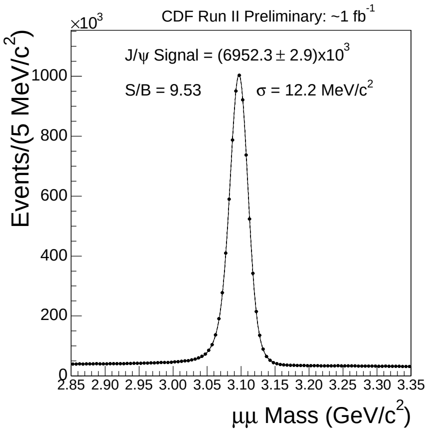

Figure 1: The $J/\psi \to \mu^+\mu^-$ invariant mass distribution. Events within a mass range of ± 50 MeV/c^2 around the central J/ψ mass value were used for both the lifetime and cross section analysis.

In addition to the di-muons from the J/ψ decay, we require a third track that is matched to the same vertex as the J/ψ. This third track can be from any of three samples of interest: $B_c^+ \to J/\psi l^+$X decays, $B^+ \to J/\psi K^+$ decays, or just $J/\psi + track$ decays. The last sample represents sources of backgrounds to the B_c^+ semileptonic decay.

5. The B_c^+ backgrounds overview

5.1. Common for both analysis

Both the lifetime and cross section analysis have some common sources of background: misidentified J/ψ, misidentified third muons, and $b\bar{b}$ backgrounds. The misidentified J/ψ background occurs when one of the muons is actually a mis-reconstructed hadron or muon from other sources that produce a mass consistent with that of the J/ψ. The misidentified third muon background can arise from the following sources. The J/ψ in the $J/\psi + track$ system is highly populated by non-B_c^+ sources. The third track associated with the J/ψ could be a π^+ or K^+ that can either decay-in-flight or punch-through the calorimeter and the steel absorber and produce the muon signature. The $b\bar{b}$ events represent cases when a J/ψ is produced from one b jet and the third muon originates from the other b in same event.

Figure 2 shows the misidentified muon rates for $\pi^\pm$, $K^\pm$, and p($\bar{p}$) and the pseudo-proper decay length ct* for misidentified third muons.

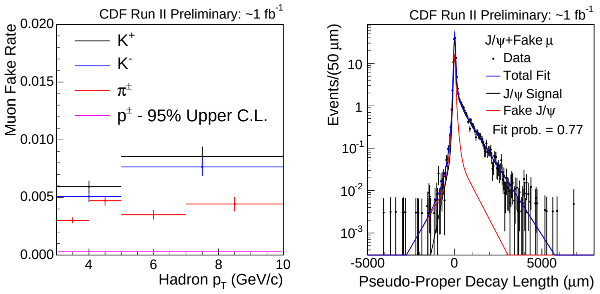

Figure 2: The misidentified muon rates from $\pi^\pm$, $K^\pm$, and p($\bar{p}$) as a function of hadron p_T (left), and the pseudo-proper decay length ct* for misidentified third muons (right).

5.2. Specific for each analysis

There is an additional background for the cross section measurement. The selected $B_c^+ \to J/\psi\mu^+X$ sample contains contributions from other B_c^+ decays with a tri-muon in the final state. For example, a B_c^+ can decay into $\psi(2S)\mu^+\nu$ followed by $\psi(2S) \to J/\psi X$.

The following backgrounds are specific to the lifetime analysis: misidentified e$^\pm$, residual conversions, and prompt J/ψ. The misidentified e$^\pm$ can arise from cases when a $\pi^\pm$, K$^\pm$, or $\bar{p}$ from the $J/\psi + track$ system satisfies the e$^\pm$ likelihood function based on the calorimeter responses. The residual conversions are e$^\pm$ from γ-conversion or π^o Dalitz decays. The prompt J/ψ are additional $J/\psi l^\pm$ candidates where the J/ψ originates from prompt non-B_c^+ sources. Figure 3 illustrates the e^+e^- veto efficiencies and the pseudo-proper decay length ct* distribution for the J/ψ+Conversion e background sample.

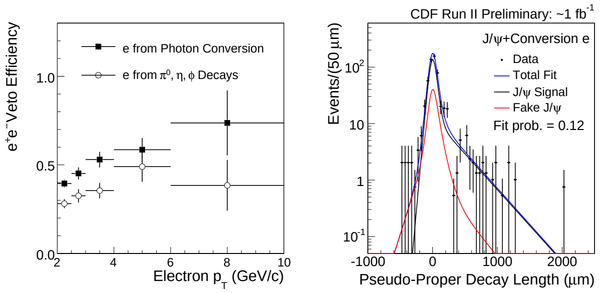

Figure 3: The e^+e^- veto efficiencies as a function of electron p_T (left), and the pseudo-proper decay length ct* distribution for the J/ψ+Conversion e background sample (right).

6. The B_c^+ lifetime results

6.1. Lifetime systematic uncertainties

The systematic uncertainties in the B_c^+ lifetime measurement originate from uncertainties in our models for background and signal events. Some of the largest systematic uncertainties are summarized below:

- Resolution function - choice of model for detector resolution: $\pm 3.8\ \mu m$
- Pythia model for $b\bar{b}$ background - relative contribution of QCD processes: $\pm 2.4\ \mu m$
- Vertex detector alignment - uncertainties in the positions of silicon detectors: $\pm 2.0\ \mu m$
- e^+e^- veto efficiency - uncertainties related to modeling e^+e^- veto efficiencies: $\pm 1.5\ \mu m$
- B_c spectrum - variations of the K factor distribution due to variations in the B_c production spectrum: $\pm 1.3\ \mu m$

We add the individual uncertainties in quadrature to obtain a total uncertainty of $\pm 5.5\ \mu m$.

6.2. Lifetime results

We fit the ct^* distributions for signal candidates in the $J/\psi\mu^+$ and $J/\psi e^+$ channels separately using likelihood functions based on our models for signal and background events. The fitted data is shown in Fig. 4 for $B_c^+ \to J/\psi\mu^+X$ and for $B_c^+ \to J/\psi e^+X$ decays.

The B_c^+ lifetime is found to be $179.1^{+32.6}_{-27.2}$(stat) μm for the $J/\psi\mu^+$ final state and $121.7^{+18.0}_{-16.3}$ (stat) μm for the $J/\psi e^+$ decay mode, respectively. We performed the simultaneous fit of both samples and found an average B_c^+ lifetime of $142.5^{+15.8}_{-14.8}(stat) \pm 5.5(syst)\ \mu m$. Figure 5 shows our B_c^+ average lifetime comparison with other measurements.

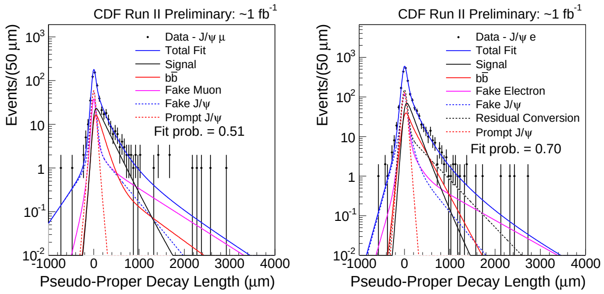

Figure 4: The pseudo-proper decay length ct* distributions for $B_c^+ \to J/\psi\mu^+X$ decays (left) and for $B_c^+ \to J/\psi e^+X$ decays (right) with their the background models superimposed.

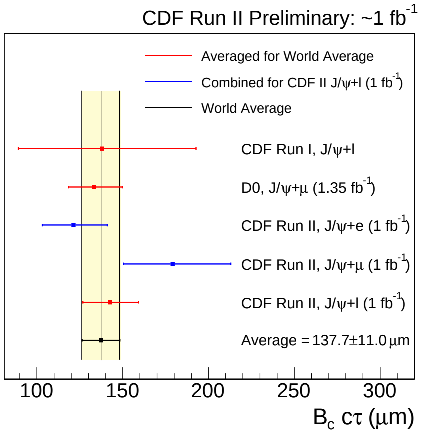

Figure 5: World average of B_c^+ lifetime, which includes the CDF Run I B_c lifetime, the most recent D0 Run II result, and the result presented in this paper. The lifetimes are weighted by the total variance of the individual measurements in the average.

7. The B_c^+ relative cross section

In order to measure the B_c^+ relative cross section we need to find the numbers of B_c^+ and B^+, $N(B_c^+)$ and $N(B^+)$, and determine the relative efficiency, $\epsilon_{rel} = \epsilon(B^+)/\epsilon(B_c^+)$. We select 229 (214) B_c^+ candidates with the requirement $p_T(B_c^+) > 4$ (6) GeV/c, respectively. The number of B_c^+ signal events after backgrounds subtraction is presented in the following subsection. The number of $B^+ \to J/\psi K^+$ signal events is found to be 2333 ± 55 (2299 ± 53) for $p_T(B^+) > 4$ (6) GeV/c, respectively. The combinatoric and $B^+ \to J/\psi\pi^+$ contributions are subtracted.

7.1. The B_c^+ backgrounds and excess

The backgrounds and the resulting number of signal events for the $B_c^+ \to J/\psi\mu^+\nu$ decays are summarized in Table I. The background identified as "Doubly misidentified" in Table I represents the subsample of misidentified J/ψ and misidentified third muons that needs to be subtracted only once to avoid double counting.

Table I Observed $N(B_c^+ \to J/\psi\mu^+\nu)$ for the $p_T(J/\psi\mu) >$ 4 GeV/c (6 GeV/c) threshold.

	$p_T(B) > 4$ GeV/c	$p_T(B) > 6$ GeV/c
$N(B_c^+)$ observed	229±15.1(stat)	214±14.6(stat)
Misidentified J/ψ	21.5±3.3(stat)	20.5±3.2(stat)
Misid. third muon	55.8±2.0(stat)	53.6±1.9(stat)
Doubly misid.	-8.8±0.4(stat)	-7.5±0.3(stat)
$b\bar{b}$ background	37.7±7.3(st+sys)	35.4±7.0(st+sys)
Other B_c^+ modes	5.2±0.5(stat)	4.8±0.4(stat)
Total background	111.4±8.3(stat)	106.9±8.0(stat)
B_c^+ signal	117.6±17.2(stat)	107.1±16.7(stat)

Figure 6 shows the invariant mass distribution of the $B_c^+ \to J/\psi\mu^+X$ data events with the experimental backgrounds and a Monte Carlo simulation of the signal sample superimposed (left), and with the background subtracted (right).

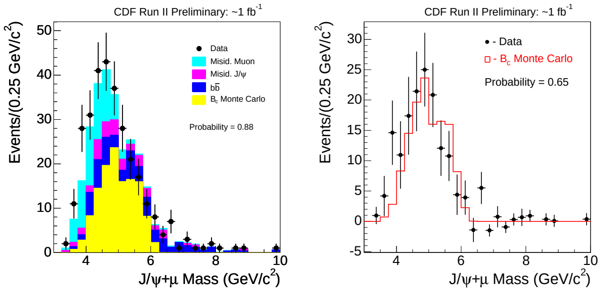

Figure 6: The invariant mass distribution of the $B_c^+ \to J/\psi\mu^+X$ data events with the experimental backgrounds and a Monte Carlo simulation of the signal sample superimposed (left), and with the background subtracted applied (right).

7.2. The relative efficiency ϵ_{rel}

In order to determine the relative efficiency, we simulate $B^+ \to J/\psi K^+$, $B_c^+ \to J/\psi\mu^+\nu$, and $B_c^{*+} \to B_c^+\gamma$ decays. As a description of the $\eta - p_T$ spectrum for B_c^+ we use the most recent theoretical work by Chang *et al.* [3]. For the B^+ we used the spectrum from Ref. [7], which is found to be in good agreement with CDF measurements. All Monte Carlo simulation events are passed through the full detector and trigger simulation. The Monte Carlo simulation samples were processed in the same way as for the data. The efficiencies $\epsilon_{B_c^+}$ and ϵ_{B^+} for $p_T(B) > 4$ (6) GeV/c, along with the relative efficiency, are presented in Table II.

Table II Efficiencies for B_c^+ and B^+ for $p_T(B) > 4$ (6) GeV/c.

Efficiency	$p_T(B) > 4$ GeV/c	$p_T(B) > 6$ GeV/c
$\epsilon_{B_c^+}$ (%)	0.0551 ± 0.0010	0.1232 ± 0.0024
ϵ_{B^+} (%)	0.3231 ± 0.0022	0.6005 ± 0.0042
ϵ_{rel}	5.867 ± 0.068 (stat)	4.873 ± 0.060 (stat)

The p_T spectra for data and Monte Carlo simulation are shown in Fig. 7.

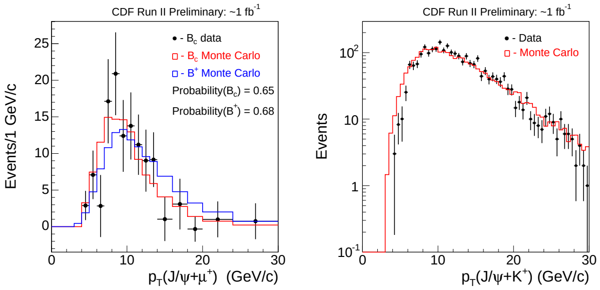

Figure 7: The comparison of the p_T spectra of data versus Monte Carlo simulation for $B_c^+ \to J/\psi\mu^+\nu$ (left), and for $B^+ \to J/\psi K^+$ decays (right).

7.3. Cross section systematic uncertainties

We divide the systematic uncertainties into two categories: uncertainties on the number of B_c^+ signal events and uncertainties in the determination of the relative efficiency.

7.3.1. B_c^+ background uncertainty

The systematic uncertainty considered in the determination of $N(B_c^+)$ arise from events which do not originate from B_c^+ decays. All backgrounds are assigned a systematic uncertainty except the misidentified J/ψ background. Since the estimation of this background is determined directly from the sidebands of the J/ψ, we do not know of any source of systematic error that should be included.

The largest source of uncertainty in the misidentified third muon calculation is due to the poor knowledge of the proton fraction in the $J/\psi + track$ sample. The particle identification method, dE/dx, does not allow us to separate protons from kaons in our kinematic region. Consequently, we measure the proton fraction in other momentum ranges using the time-of-flight (TOF) particle identification combined with dE/dx information and then extrapolate the fraction to our momentum range according to measured trends in Monte Carlo simulation.

The other $N(B_c^+)$ systematic uncertainty arises from a poor knowledge of non-exclusive $B_c^+ \rightarrow J/\psi\mu^+X$ branching ratios and is estimated by varying the branching ratios of eleven B_c^+ decay modes that may contribute to the sample of tri-muon events. In order to assign a systematic uncertainty we double and halve the branching ratios of the non-exclusive decays with respect to the rate of $B_c^+ \rightarrow J/\psi\mu^+\nu$. We choose the larger variation in either direction for the systematic uncertainty.

Table III summarizes all of the B_c^+ background systematic uncertainties assigned.

Table III Systematic uncertainties on the number of $B_c^+ \rightarrow J/\psi\mu^+\nu$ events for different $p_T(B)$ thresholds. The total uncertainty is calculated by adding all the individual uncertainties in quadrature.

$N(B_c^+)$ uncertainties	$p_T(B) > 4$ GeV/c	$p_T(B) > 6$ GeV/c
Misid. third muon	±5.7 (sys)	±5.5 (sys)
Doubly misid.	±0.9 (sys)	±0.8 (sys)
Other B_c^+ decays	$^{+6.0}_{-2.8}$ (sys)	$^{+5.6}_{-2.5}$ (sys)
Total	$^{+8.3}_{-6.4}$ (sys)	$^{+7.9}_{-6.1}$ (sys)

7.3.2. Relative efficiency systematic uncertainty

We consider the systematic uncertainty in the prediction of the relative efficiency due to the measured statistical uncertainty of the B_c^+ lifetime, knowledge of the production spectra for B_c^+ and B^+, and differences between K and μ triggering rates at the first level of the CDF trigger system, the extremely fast trigger, XFT.

The relative efficiency systematic uncertainty due to B_c^+ lifetime uncertainty is estimated by varying the lifetime by ±14 μm of its default value. This variation represents approximately one standard deviation in the average lifetime result.

The relative efficiency systematic uncertainty due to the knowledge of B_c^+ p_T spectrum is fully based on the theoretically predicted p_T spectra from work in Ref. [3]. We consider the variations between:

- doubling the $q\bar{q}$ contribution relative to the nominal approach;
- the pure gluon fusion model, called the fixed flavor number (FFN) model, and the more complete $gg + g\bar{b} + gc$ model, known as the general-mass variable-flavor-number (GMVFN) model;
- the combined $B_c^+ + B_c^{*+}$ spectrum and a pure B_c^+ spectrum.

The systematic uncertainty due to knowledge of the B^+ p_T spectrum is estimated by varying the Monte Carlo simulated spectrum below 10 GeV/c to bring it into agreement with the data (see the right plot in Fig. 7. The difference between the nominal and recalculated relative efficiency is assigned as the uncertainty due to B^+ p_T spectrum.

Another source of systematic uncertainty that we consider is the different XFT efficiencies of kaons and muons that exist in the data and are not modeled in the simulation.

The total ϵ_{rel} systematic uncertainty is summarized in Table IV.

Table IV Systematic uncertainty assigned to ϵ_{rel} for different $p_T(B)$ thresholds. The numbers 0.720 and 0.298 in the "Total" represent the uncertainties due to of B_c^+ spectrum.

ϵ_{rel} uncertainties	$p_T(B) > 4$ GeV/c	$p_T(B) > 6$ GeV/c
B_c^+ lifetime	$^{+0.393}_{-0.223}$	$^{+0.354}_{-0.160}$
B_c^+ spectrum	$\pm$ 0.720	$\pm$ 0.298
B^+ spectrum	$\pm$ 0.340	$\pm$ 0.161
XFT systematics	$\pm$ 0.192	$\pm$ 0.160
Total	$^{+0.554}_{-0.450}\pm0.720$	$^{+0.420}_{-0.278}\pm0.298$

8. The B_c^+ relative cross section results

We have performed a measurement of the relative production cross section of $B_c^+ \rightarrow J/\psi\mu^+\nu$ in inclusive J/ψ data with an integrated luminosity of 1 fb^{-1}. We have identified a sample of 229 (214) events with an estimated background from all sources of 111 ± 8 (107 ± 8) events for $p_T(J/\psi\mu^+) > 4$ (6) GeV/c, respectively. The final numbers used in the cross section measurement, including systematic uncertainties, are given in Table V.

We give the result for the ratio $\frac{\sigma(B_c^+)BF(B_c^+\rightarrow J/\psi\mu^+\nu)}{\sigma(B^+)BF(B^+\rightarrow J/\psi K^+)}$ with $p_T(B) > 4$ GeV/c thresholds as

$$0.295 \pm 0.040\ (\text{stat.})^{+0.033}_{-0.026}\ (\text{syst.}) \pm 0.036\ (p_T\ \text{spec})$$

and for $p_T(B) > 6$ GeV/c as

$$0.227 \pm 0.033\ (\text{stat.})^{+0.024}_{-0.017}\ (\text{syst.}) \pm 0.014\ (p_T\ \text{spec}).$$

Of the two results, the measurement with the $p_T(B) > 6$ GeV/c threshold has the lower systematic error. Below 6 GeV/c there is uncertainty in the B^+

Table V Final numbers used in the calculation of the relative $B_c^+ \to J/\psi\mu^+\nu$ production cross section times the branching ratio for two different $p_T(B)$ thresholds.

Final values	$p_T(B) > 4$ GeV/c
$N(B_c^+)$	117.6±17.2 (stat) ${}^{+8.3}_{-6.4}$(sys)
$N(B^+)$	2333± 55 (stat)
ϵ_{rel}	5.867±0.068 (stat) ${}^{+0.554}_{-0.450}$(sys) ±0.720 (B_c^+ spectrum)
Final values	$p_T(B) > 6$ GeV/c
$N(B_c^+)$	107.2±16.7 (stat) ${}^{+7.9}_{-6.1}$ (sys)
$N(B^+)$	2299±53 (stat)
ϵ_{rel}	4.872±0.060 (stat) ${}^{+0.420}_{-0.278}$ (sys) ±0.298 (B_c^+ spectrum)

efficiency that appears to introduce a significant systematic discrepancy between the simulated spectrum and the spectrum as determined from the data.

Using theoretical assumptions and independent measurements, we are then able to calculate the total B_c^+ cross section. Using the measured quantities $BR(B^+ \to J/\psi K^+) = (1.007 \pm 0.035) \times 10^{-3}$ [8] and $\sigma(B^+) = 2.78 \pm 0.24$ μb for $p_T(B^+) > 6$ GeV/c [4], we calculate

$$\sigma(B_c^+) * BR(B_c^+ \to J/\psi\mu^+\nu) = 0.64 \pm 0.20 \text{ nb}$$

for $p_T(B_c^+) > 6$ GeV/c. Assuming that the branching ratio $BR(B_c^+ \to J/\psi\mu^+\nu) = 2.07 \times 10^{-2}$ [9], we find the total B_c^+ cross section to be

$$\sigma(B_c^+) = 31 \pm 10 \text{ nb}$$

9. Conclusions

We have performed measurements of the B_c^+ lifetime and production properties based on semileptonic $B_c^+ \to J/\psi + l^+ + X$ decays using data from $p\bar{p}$ collisions collected with the CDF II detector corresponding to an integrated luminosity of 1 fb^{-1} at $\sqrt{s}$=1.96 TeV.

References

[1] Reference to a particular charge state also implies the charge conjugate state.

[2] S. Godfrey, Phys. Rev. D **70**, 054017 (2004); V.V.Kiselev, arXiv:hep-ph/0308214.

[3] Chao-Hsi Chang, Phys. Rev. D **72**, 114009 (2005).

[4] A.Abulencia *et al.* (CDF Collaboration), Phys. Rev. D **75**, 012010 (2007).

[5] A.Abulencia *et al.* (CDF Collaboration), Phys. Rev. Lett. **97**, 012002 (2006).

[6] T.Aaltonen *et al.* (CDF Collaboration), Phys. Rev. Lett. **100**, 182002 (2008).

[7] M. Cacciari *et al.,* J. High Energy Phys. **07**, 033 (2004).

[8] C. Amster *et al.* (Particle Data Group), Phys. Lett. **B667**, 1 (2008).

[9] M.A. Ivanov *et al.,* Phys. Rev. D **73**, 054024 (2006).